CHARACTERIZATION OF MICRO-DOMAIN STRUCTURE OF SOLVENT-SWOLLEN COAL BY SMALL ANGLE NEUTRON SCATTERING AND PROTON SPIN DIFFUSION

Koyo NORINAGA*, Masashi IINO, and George D. CODY†
Institute for Chemical Reaction Science, Tohoku University
Katahira, Aoba-ku, Sendai, 980-8577, Japan
†*Geophysical Laboratory, Carnegie Institution of Washington*
5251 Broad Branch Road, Washington, D. C. 20015

KEYWORDS: Coal, Swelling, Microphase separation

ABSTRACT

Blind Canyon coal was swollen by deuterated pyridine and was subjected to small angle neutron scattering (SANS) and ^{1}H NMR relaxation measurements. Based on the transverse relaxation characteristics, it was found that there exist at least two distinct structural regions in the swollen coals. However the measured longitudinal relaxation was best characterized by a single component as spin diffusion is rapid in the swollen coals. The dynamics of spin diffusion were revealed using a partially modified Goldman-Shen pulse sequence and analyzed by a simple mathematical model of a two phase system. The *interdomain spacing*, d_i, was estimated based on the diffusive path length for each spatial dimension. The d_i value evaluated under one-dimension was 15 nm and agreed with d_i determined by SANS, suggesting that the domain shape is sheet.

INTRODUCTION

The most convincing model of coal structure is that of a cross-linked macromolecular network. [1-5] The swelling of coal in various solvents has been studied to evaluate the molecular weight between cross-link points. [2, 4-8] The *Flory-Rehner theory* [9] has been frequently employed to relate the macromolecular network parameters to the degree of swelling in a good solvent. The theory assumes that the deformation is affine, i.e., the primitive chain is deformed in the same way as the macroscopic deformation (swelling) of the sample. Accordingly, the coal must swell uniformly in the segmental scale when we relate the macroscopic swelling to molecular characteristics such as the cross-link density. Based on the ^{1}H NMR transverse relaxation characteristics, however, it was found that the coal hydrogen in the pyridine-swollen state could be divided into two groups: those with relaxation characteristic of solids and those with relaxation characteristic of liquids. [10-17] Barton et al. [12] reported that up to 60 % of coal's macromolecular structure becomes mobile when immersed in deuteropyridine, while the remaining 40 % remains rigid as detected through ^{1}H NMR transverse relaxation measurements. Base on this finding, they first established that the swollen coal has a phase separated structure involving a solvent rich phase and an apparently solvent impervious phase.

Recently, Norinaga et al. [18] reported that the scale of the heterogeneity in the swollen coals. They characterized the phase separated structure of solvent swollen coal using its proton spin diffusion property. Five coals of different ranks were swollen by saturation with deuterate pyridine and were subjected to ^{1}H NMR relaxation measurements. The dynamics of spin diffusion were revealed using a partially modified Goldman-Shen pulse sequence and analyzed by a simple mathematical model of a two phase system. These calculations indicated that the solvent rich phase domains in the swollen coals range in size from several up to 20 nm. These results highlight the current limits in our understanding of the macromolecular structure of coals and place into question the use of affine models of strain for the interpretation of macroscopic swelling measurements. However the results depend on the spatial dimension of domains, i.e., the degree of freedom of the spin diffusion. Hence the information regarding the morphology of the domains is required to evaluate the domain size more precisely.

In the present study, the phase structure of a bituminous coal swollen by deuterate pyridine was characterized. In order to evaluate the morphology of the domains, we employ two different techniques. One is proton spin diffusion and the other is small angle neutron scattering(SANS). SANS gives an information on the average periodicity of the microphase structure, that is, the average distance between the centers of adjacent solvent-impervious-domains. It is possible to convert the size of the solvent rich phase into an interdomain spacing using an appropriate domain model. Thus the morphology of the domains can be evaluated by comparing the results of the spin diffusion with those of SANS.

EXPERIMENTAL

Samples. Blind Canyon coal supplied from Argonne Premium Coal Sample suite was used. The elemental composition of the dried Blind Canyon coal (hereafter referred to as BL) was C=80.7 wt %, H=5.8 wt %, N=1.6 wt %, S=0.4 wt %, and O=11.6 wt % on a dry-ash-free basis. [19] Their particle sizes were finer than 150 μm. 0.3 g of BL was weighed and transferred to an NMR tube with a 10 mm o.d. This tube was charged with per-deutero pyridine (Aldrich, 99.99% atom D), py-d_5, and sealed under a pressure of less than 2 Pa while frozen in liquid nitrogen. Solvent to coal mass ratio (S/C) ranged from 0.36 to 4.12. BL was exhaustively extracted in pyridine prior to SANS experiments. 0.15 g of sample

was loaded into a suprasil cyrindrical cell with 2 mm path length (vol = 0.7 mL). 0.6 mL of deuterated solvent (benzene / pyridine mixed solvent) was introduced to the cell.

SANS. SANS data were measured at the Intense Pulsed Neutron Source of Argonne National Laboratory, using the Small Angle Diffractometer (SAD). This instrument uses pulsed neutrons derived from spallation with wavelengths in the range of 0.1 - 1.4 nm and a fixed sample-to-detector distance of 1.54 m. The scattered neutrons are measured using a 64 x 64 array of position sensitive, gas filled, 20 x 20 cm^2, proportional counters with the wavelengths measured by time of flight by binning the pulse to 67 constant $\Delta t/t = 0.05$ time channels. The size range in a SANS experiment is constrained by both the geometry of the instrument and the wavelength of the neutrons which determine the working range of momentum transfer Q.

$$Q=4\pi\lambda^{-1}\sin\theta \qquad (1)$$

where θ is half the Bragg scattering angle and λ is the wavelength of the neutrons. Given the characteristics of the SAD at the Intense Pulsed Neutron Source (IPNS), useful SANS data in the Q range of 0.0006-0.025 nm^{-1} can be obtained in a single measurement. The reduced data for each sample is corrected for the backgrounds from the instrument, the suprasil cell, and the solvent as well as for detector nonlinearity. Data are presented on an absolute scale by using the known scattering cross-section of a silica gel sample.

^{1}H NMR. NMR measurements were carried out at 303 K using a JEOL Mu-25 NMR spectrometer equipped with a spin locking unit operating at a proton resonance frequency of 25 MHz. The solid-echo pulse sequence, [20] $90°_x$-τ-$90°_y$ (90° phase shift) provided an approximation to the complete free induction decay (FID). Typical values for the pulse width, pulse spacing, repetition time and number of scans were 2.0 μs, 8.0 μs, 6 s, and 32, respectively. The saturation recovery pulse sequence, $90°_x$-τ-$90°_x$, was used to monitor the recovery of the magnetization with the pulse separation time, τ and provided T_1. $T_{1\rho}$ was measured using a spin-locking pulse sequence, [21] that includes a $90°_x$ pulse followed by a reduced amplitude pulse, phase shifted 90°, and sustained for a variable time, t. The magnetization remaining at time t is monitored by observation of the free induction decay signal. The rotating frame measurements were made in a 6 G radiofrequency field. The spin diffusion was monitored with the Goldman-Shen pulse sequence. [22] In order to avoid the dead-time effect after the pulse, the original pulse sequence was modified as $90°_x$-τ_0-$90°_x$-t-$90°_x$-τ_1-$90°_y$, according to Tanaka and Nishi. [23]

RESULTS AND DISCUSSION

SANS results. The SANS data for a number of solutions of varying benzene to pyridine are presented in Figure 1. These data are presented as the log of the coherent scattering intensity, $I(Q)$, against the log of the momentum vector, Q. It is clear that there are significant changes in coherent scattering with increasing swelling ratio. These changes are relatively large scale. For example in the intermediate Q range around 0.02, $I(Q)$ increases by a factor of five with increased swelling (pyridine concentration in solution). It should be noted that Q~0.02 corresponds to a real space length of ~16 nm. It is noteworthy that at low Q, the effects of swelling are considerably less, thus the changes in coherent scattering "peak" in the intermediate Q range. Cody et al. [24] observed that similar creation of scattering intensity in the intermediate Q range with swelling of the Upper Freeport coal. In that work, they argued that the scattering at low Q was independent of scattering at intermediate Q. Thus, we concluded that the intermediate scattering was the results of an interparticle scattering phenomena as opposed to primary scattering of individual particles. The same interpretation can be applied here since the swelling of this coal is inhomogeneous, i.e., there exist solvent rich and solvent impervious domains as will be demonstrated by the ^{1}H NMR relaxation characteristics.

^{1}H NMR results. The FID curves for the swollen BL coal are drawn as a function of decay time in Figure 2. Although the solvent swelling enhances the fraction of slowly decaying components, a portion of the coal hydrogen remains rigid. For a dipole coupled rigid systems such as dry coal, the time decay of the nuclear magnetization can be characterized by a Gaussian function. On the other hand, in a liquid or a liquid-like environment, the magnetization decay is approximately an exponential function. Therefore the observed FID was assumed to be expressed by the following equation and was analyzed numerically by the nonlinear least squares method.

$$I(t) = I_G(0)\exp[-t^2/2T_{2G}^2] + I_{L1}(0)\exp[-t/T_{2L1}] + I_{L2}(0)\exp[-t/T_{2L2}] \qquad (2)$$

where $I(t)$ and $I_i(t)$ are the observed intensity at time t, and that attributed to component i, respectively, and T_{2i} is the transverse relaxation time of the i th component. The fractions of hydrogen producing exponential decays, f_{MH}, are plotted against S/C in Figure 3. f_{MH} was increased up to 0.5 with increase in S/C. However, f_{MH} kept almost constant value above S/C≈2.24, indicating that there exist the solvent impenetrable regions in the swollen coal even at S/C=4.72. For the swollen coal samples, it is clear that there are domains which do not swell and are not penetrated by solvent as shown schematically in Figure 4. The phase structures of the swollen coal are separated into at least two phase, i.e., solvent rich (SR)

and solvent impervious phase (SI).

To examine whether the spin diffusion process is active or not in the swollen coal samples, proton longitudinal relaxation was measured both in the laboratory and rotating frame. Table 1 lists the result of T_1 and $T_{1\rho}$ measurement for the swollen UF coal. T_1 is composed of one component while $T_{1\rho}$ can be analyzed by the sum of two exponential functions. From these results, one can clearly understand the effect of spin diffusion. T_2 signals are composed of three components without the effect of spin diffusion while $T_{1\rho}$ and T_1 measurements are affected strongly by spin diffusion and the number of the components decreases from $T_{1\rho}$ to T_1. The existence of at least two time constants for a rotating frame longitudinal relaxation process i.e., $T_{1\rho}$, in a system means that spin-diffusion processes cannot effectively average the different dynamical properties of protons in different spatial domains on the relevant time scale of the specific relaxation process. On the other hand, in the time scale of T_1 measurements, the distinctly separated spin systems were sufficiently averaged by the spin diffusion. The scale of spatial heterogeneities of the swollen coals can be estimated by evaluating the diffusive path length, i.e., the maximum linear scale over which diffusion is effective. The Goldman-Shen pulse sequence was thus employed to monitor the spin diffusion process. The advantage of the Goldman-Shen experiment is that the time for spin diffusion can be arbitrarily varied, and if this time is much less than T_1, the analysis is straightforward. The Goldman-Shen experiment is a technique to put the separate spin systems at different spin temperatures and then sample them as a function of time so that their approach to equilibrium can be followed. In Figure 5, the recovery factor of the magnetization of SI phase, $R(t)$, is plotted versus square root of time, $\tau^{1/2}$ for the solvent-swollen BL coals. S/C has almost no effects on the observed $R(t)$. The time evolution of $R(t)$ is analyzed by the diffusion equation solved by Cheung and Gerstein [25] to get information on the diffusive path length, l. The solid curves in Figure 5 represent the nonlinear least squares fits to the data by using the diffusion equation. The analytical fits give l to be 7, 16, and 25 nm for one, two, and three dimensions, respectively.

Comparison of SANS and ^{1}H NMR results. To compare the NMR results with SANS, we must convert the spin diffusion path length into an interdomain spacing. The spheres of SI phase are assumed to be covered with a uniform layer of SR phase of thickness l as shown in Figure 6. This model allowed to produce the following two equations,

$$l = r_C - r_{SI} \tag{3}$$

$$\phi_{SI} = \phi_C(1 - f_{MH}) = \left(\frac{r_{SI}}{r_C}\right)^d \tag{4}$$

where ϕ_{SI}, ϕ_C, and d are volume fractions of SI domains, volume fraction of coal in the swollen coal gel, and spatial dimension of the domain, respectively. In eq 4, we assumed that the hydrogen ratio is identical to the volume ratio. Twice r_c is taken to be equal to the interdomain spacing, d_i. d_i was estimated for each spatial dimension. The d_i evaluated under one-dimension at S/C=4 was approximately 15 nm and agreed with d_i determined by SANS, suggesting that the domain shape is sheet.

ACKNOWLEDGMENT. The authors are grateful to Drs. Tadashi Yoshida and Masahide Sasaki of the Hokkaido National Industrial Research Institute for their useful advice on the NMR measurements. This work was supported in part by a "Research for the Future Project" grant from the Japan Society for the Promotion of Science (JSPS), through the 148th Committee on Coal Utilization Technology.

REFERENCES

(1) van Krevelen, D. W. *Fuel* **1966**, *45*, 229.
(2) Green, T.; Kovac, J.; Brenner, D.; Larsen, J. W. In *Coal Structures*; Mayers,R. A., Ed.; Academic Press: New York, 1982.
(3) Brenner, D. *Fuel* **1985**, *64*, 167.
(4) Larsen, J. W.; Green, T. K.; Kovac, J. *J. Org. Chem.* **1985**, *50*, 4729.
(5) Lucht, L. M.; Peppas, N. A. *Fuel* **1987**, *66*, 803.
(6) Sanada, Y.; Honda, H. *Fuel* **1966**, *45*, 295.
(7) Kirov, N. Y.; O'Shea, J. M.; Sergeant, G. D. *Fuel* **1968**, *47*, 415.
(8) Nelson, J. R. *Fuel* **1983**, *62*, 112.
(9) Flory, P. J. *Principles of Polymer Chemistry*; Cornell University Press: Ithaca: NY 1953.
(10) Jurkiewicz, A.; Marzec, A.; Idziak, S. *Fuel* **1981**, *60*, 1167.
(11) Jurkiewicz, A.; Marzec, A.; Pislewski, N. *Fuel* **1982**, *61*, 647.
(12) Barton, W. A.; Lynch, L. J.; Webster, D. S. *Fuel* **1984**, *63*, 1262.
(13) Kamienski, B.; Pruski, M.; Gerstein, B. C.; Given, P. H. *Energy Fuels* **1987**, *1*, 45.
(14) Jurkiewicz, A.; Bronnimann, C. E.; Maciel, G. E. *Fuel* **1990**, *69*, 804.
(15) Jurkiewicz, A.; Bronnimann, C. E.; Maciel, G. E. High-Resolution ^{1}H NMR studies of Argonne premium coals. In *Magnetic Resonance in Carbonaceous Solids*; Botto, C. E., Sanada, Y., Eds.; Advances in Chemistry; American Chemical Society: Washington, DC, **1993**, *229*, 401.

(16) Yang, X.; Larsen, J. W.; Silbernagel, B. G. *Energy Fuels* **1993**, *7*, 439.
(17) Yang, X.; Silbernagel, B. G.; Larsen, J. W. *Energy Fuels* **1994**, *8*, 266.
(18) Norinaga, K.; Hayashi, J. i.; Chiba, T.; Cody, G. D. *Energy Fuels* **1999**, *in press.*
(19) Vorres, K. S. *User's Handbook for the Argonne Premium Coal Sample Program*; Argonne National Laboratory: Argonne: IL, 1993.
(20) Powles, J. G.; Mansfield, P. *Phys. Lett.* **1962**, *2*, 58.
(21) Hartmann, S. R.; Hahn, E. L. *Phys. Rev.* **1962**, *128*, 2042.
(22) Goldman, M.; Shen, L. *Phys. Rev.* **1966**, *144*, 321.
(23) Tanaka, H.; Nishi, T. *Phys. Rev. B* **1986**, *33*, 32.
(24) Cody, G. D.; Obeng, M.; Thiyagarajan, P. *Energy Fuels* **1997**, *11*, 495.
(25) Cheung, T. T. P.; Gerstain, B. C. *J. Appl. Phys.* **1981**, *52(9)*, 5517.

Table 1 Results of Proton Longitudinal Relaxation Measurements for Blind Canyon Coal Swollen in Deuterated Pyridine.

S/C [a]	$T_{1\rho}$[ms]		T_1[ms]
	$T_{1\rho}^{f}$ [b]	$T_{1\rho}^{s}$ [c]	
0	0.7(0.52)	4.8(0.48)	66(1.00)
0.36	-	-	65(1.00)
0.68	1.0(0.52)	5.7(0.48)	108(1.00)
1.03	1.3(0.59)	7.3(0.41)	104(1.00)
1.33	0.8(0.67)	5.3(0.33)	112(1.00)
1.67	1.7(0.62)	12.1(0.38)	128(1.00)
2.24	1.7(0.54)	12.9(0.46)	141(1.00)
2.57	1.8(0.55)	15.8(0.45)	145(1.00)
3.52	1.7(0.54)	16.1(0.46)	130(1.00)
4.72	1.8(0.52)	20.2(0.48)	144(1.00)

Values in parentheses; fraction of each component, [a] Mass ratio of solvent to coal [b] Fast. [c] Slow.

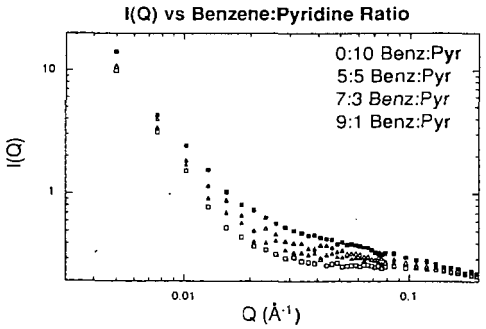

Figure 1 Coherent scattering intensity vs momentum vector for variably swollen BL residues in binary solvent of benzene-pyridine

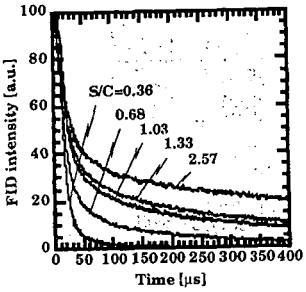

Fig.2 Transverse relaxation signals for pyridine swollen BL coal.

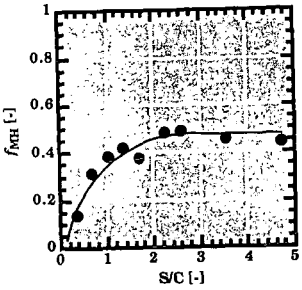

Fig.3 Change in f_{MH} with S/C.

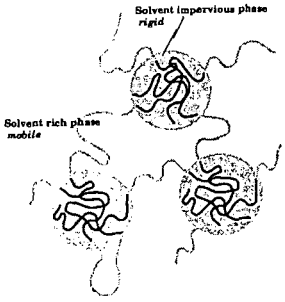

Fig. 4 Conceptual model for microdomain structure of solvent-swollen coal.

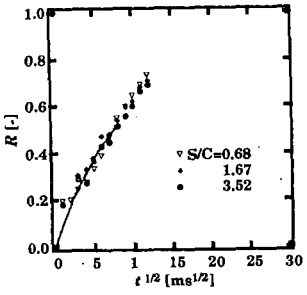

Fig.5 Recovery of proton magnetization in SI phase as a function of $t^{1/2}$ for the solvent-swollen BL coal. Solid lines represent the best fit to the data using a diffusion model.

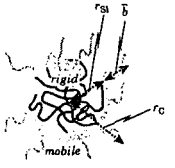

Fig.6 A 3-D domain model used to calculate the interdomain spacing from the spin diffusion distance.

SMALL ANGLE X-RAY SCATTERING STUDY OF COAL SOOT FORMATION

R. E. Winans, J. T. Parker†, S. Seifert, and T. H. Fletcher†

Chemistry Division, Argonne National Laboratory, Argonne, IL 60439
and †Chemical Engineering Department, Brigham Young University, Provo, UT 84602

Keywords: soot, SAXS, coal

ABSTRACT

The objective of this study is to examine, by small angle X-ray scattering (SAXS), the formation of soot from individual coal particle combustion in a methane flat flame burner. The SAXS instrument at the Basic Energy Sciences Synchrotron Radiation Center (BESSRC) at the Advanced Photon Source (APS) can be used to observe both the formation of spherules and clusters since it can access length scales of 6-6000 Å. The high X-ray flux enables rapid acquisition of scattering data of various regions of the flame. SAXS data reveal particle size, shape, surface areas, and surface roughness.

INTRODUCTION

Particulate formation in many types of combustion, such as in diesel engines and coal combustion, is a significant problem. For example, in coal combustion, soot formation control is important because of radiation heat transfer effects. The objective of this study is to observe in situ the formation of particles in flames using small angle X-ray scattering (SAXS). As a result of a DOE-BES Facilities Initiative (1), we have developed a high resolution SAXS instrument in the BESSRC-CAT at the Advanced Photon Source (APS). The SAXS facility offers new capabilities for measuring atomic order within disordered media, including combustion particulates, on a length scale of 6-6000 Å. A small research, flat flame burner has been constructed (2). The flux of photons from an undulator at the APS is needed to be able to observe the small number of soot particles in combustion of single coal particles.

We propose to look at the problem of particulate formation in coal combustion from the early growth stages to particulate agglomerate formation, all using SAXS. In an early in situ study (3) using SAXS to probe flames, the author noted that optical techniques had a lower limit of 600 Å while his instrument had an upper limit of 1000 Å. Typically, individual soot particles cluster to sizes starting at ~1000 Å. Optical methods can readily observe the clusters, but not the smaller spherules as they are formed. Our instrument can observe both the formation of spherules and clusters since it can access length scales of 6-6000 Å. SAXS data can reveal particle size, shape, surface areas, surface roughness and can provide information on the internal structure. This method provides complementary data to that obtained by optical methods.

Presently, a number of optical techniques are used to study soot in flames. Recently, Köylü (4) observed that there were large errors in determining soot particle size from light scattering. Also, the determination of properties were suspect due to uncertainties in soot refractive indices. However, thermophoretic sampling compiled with transmission electron spectroscopy (an ex situ method) has provided reliable size and shape information on the soot aggregates (4,5). These data can be used to help interpret the in situ SAXS results. Other optical techniques, such as laser induced fluorescence (6), have been used to analyze the pyrolysis process and especially to look at the polycyclic aromatic hydrocarbons, which are the probable precursors to soot.

A classic paper by Freltoft, Kjems, and Sinha (7) describes how power law correlations of small angle scattering can be used to describe clusters of small particles. A parameter called the fractal dimension (d_o) can be derived from this correlation. This value, d_o, relates how the mass of a cluster changes with a linear dimension. We have used this approach to examine coal derived molecules in pyridine with small angle neutron scattering data (8).

The experiments were conducted using a smaller version of a Hencken flat flame burner using a methane-air flame as the heat source. The coal particles are introduced individually through the center of the burner (5). It can be run fuel rich to observe pyrolysis or fuel lean to combust the coal particles. Other fuels, such as hydrocarbons, have been used with this burner. The burner is mounted on vertical and horizontal translation stages so that different parts of the flame can be probed.